IEEE Photonics Journal
An IEEE Photonics Society Publication

Photonic Generation and Wireless Transmission of Linearly/Nonlinearly Continuously Tunable Chirped Millimeter-Wave Waveforms With High Time-Bandwidth Product at W-Band

Volume 4, Number 1, February 2012

J.-W. Shi
F.-M. Kuo
Nan-Wei Chen
S. Y. Set
C.-B. Huang
J. E. Bowers

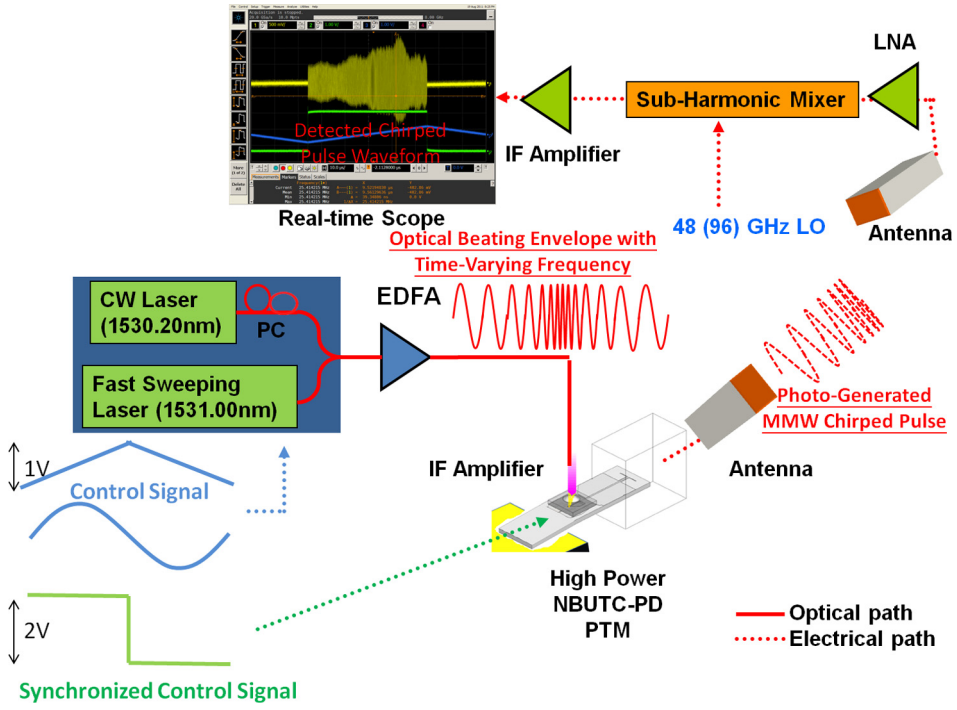

DOI: 10.1109/JPHOT.2012.2183119
1943-0655/$31.00 ©2012 IEEE

IEEE photonics SOCIETY

IEEE

Photonic Generation and Wireless Transmission of Linearly/Nonlinearly Continuously Tunable Chirped Millimeter-Wave Waveforms With High Time-Bandwidth Product at W-Band

J.-W. Shi,[1,2] F.-M. Kuo,[1,2] Nan-Wei Chen,[3] S. Y. Set,[4] C.-B. Huang,[5] and J. E. Bowers[2]

[1]Department of Electrical Engineering, National Central University, Taoyuan 320, Taiwan
[2]Electrical and Computer Engineering Department, University of California Santa Barbara, Santa Barbara, CA 93106 USA
[3]Department of Communications Engineering, Yuan Ze University, Taoyuan 320, Taiwan
[4]Alnair Labs Corporation, Tokyo 141-0031, Japan
[5]Institute of Photonics Technologies, National Tsing-Hua University, Hsinchu 300, Taiwan

DOI: 10.1109/JPHOT.2012.2183119

Manuscript received December 13, 2011; revised January 1, 2012; accepted January 3, 2012. Date of publication January 6, 2012; date of current version January 27, 2012. This work was supported by the National Science Council of Taiwan under Grant NSC-100-2918-I-008-004 and by the Defense Advanced Research Projects Agency under the MTO PICO project. Corresponding author: J. Shi (e-mail: jwshi@ee.ncu.edu.tw; jwshi@ece.ucsb.edu).

Abstract: We demonstrate a novel scheme for photonic generation of chirped millimeter-wave (MMW) pulse with ultrahigh time-bandwidth product (TBP). By using a fast wavelength-sweeping laser with a narrow instantaneous linewidth, wideband/high-power photonic transmitter-mixers, and heterodyne-beating technique, continuously tunable chirped MMW waveforms at the W-band are generated and detected through wireless transmission. Compared with the reported optical grating-based wavelength-to-time mapping techniques for chirped pulse generation, our approach eliminates the problem in limited frequency resolution of grating, which seriously limits the continuity, tunability, and TBP of the generated waveform. Furthermore, by changing the alternating current (AC) waveform of the driving signal to the sweeping laser, linearly or nonlinearly continuously chirped MMW pulse can be easily generated and switched. Using our scheme, linearly and nonlinearly chirped pulses with record-high TBPs (89–103 GHz/50 μs/7 $\times$ 10^5) are experimentally achieved.

Index Terms: Microwave photonics, microwave photonics signal processing, photodetectors.

1. Introduction

The capability to generate chirped millimeter-wave (MMW) pulses is pivotal in realizing a modern radar system with high temporal resolution [1]–[3]. A chirped pulse system avoids the saturation of high-peak voltage (current) in the electrical transmitter with a much longer pulse duration and, at the same time, offers comparable temporal resolution as compared to systems using extremely short electrical pulses ($<$ 1 ns) [1], [2]. The key figure-of-merit in evaluating a chirped waveform is its compression ratio (also known as the time-bandwidth product [TBP]), which equals to the product of sweeping MMW bandwidth (B) and the temporal pulse duration (T) [1]–[4]. A larger compression ratio means an electrical pulse with shorter duration (therefore higher temporal resolution), and

higher peak power can be obtained at the receiver end after chirp compensation. In modern real-time pulsed radar systems, the typical compression ratios are on the orders of several hundred or thousand with pulse durations around 100 μs [1]–[4]. However, the commercial all-electronic scanning microwave oscillator (yttrium iron garnet (YIG) oscillator) [5], [6] usually exhibits limited scanning bandwidth/central frequency, high driving voltage, and a slow scanning rate (1 GHz/ms) [5], [6]. For the desired pulse duration (< 100 μs), the scanning bandwidth is usually less than only 1 GHz [3], [5].

An attractive solution to generate chirped electrical waveforms is through the photonics approach [7], [8]. In various works based on incorporating time-multiplexing and high resolution pulse shapers, the ability to generate microwave waveforms with indefinite record length have been demonstrated [9]–[11]. Another scheme for photonic microwave chirped pulse generation is based on the direct frequency-to-time mapping technique [12]–[17]. Such a technique is enabled by sending a short optical pulse through a long single-mode fiber so that the accumulated quadratic spectral phase impresses a large linear chirp onto the resulting time-domain waveform. The desired chirped microwave pulse is therefore a scaled replica of the optical spectrum. The shape, frequency-sweeping range of the chirped microwave waveform can therefore be arbitrarily defined using a pulse shaper [12], [13], special designed fiber Bragg grating (FBG) [14], [15], or an electrooptical intensity modulator [16], [17]. In a very recent work, chirped MMW pulses with a high central frequency of 40 GHz and a wide scanning range (10 to 55 GHz) have been experimentally demonstrated with pulse durations around 1.2 ns [15]. In that work, the corresponding pulse compression ratio of 50 is severely limited by the optical pulsewidth. To obtain a higher compression ratio, further extending the optical pulsewidth to the microsecond level would require a much lower (kHz) laser repetition rate. Furthermore, a true linear pulse chirp is difficult to achieve in practical Fourier-transform pulse shaper systems due to the finite pixelation of the spatial light modulator.

In this paper, a novel scheme for photonic generation of chirped MMW pulse with ultrahigh TBP is proposed. Through the use of a broadband photonic transmitter [18]–[21] and a special designed wavelength-swept laser with a narrow instantaneous linewidth, we experimentally demonstrate and in-detail analyze a novel photonic technique for generation, wireless transmission, and detection of a truly continuous chirped MMW pulse [22]. By simply changing the driving signal of wavelength-sweeping laser, linearly or nonlinearly chirped MMW pulses covering the W-band (89–103 GHz) with record-high TBP (14 GHz, 50 μs, 7×10^5) are achieved.

2. Device Structure and Fabrication

Fig. 1 shows the schematic of our experimental setup. The optical MMW signal is simply generated by the heterodyne-beating technique. A wavelength-sweeping laser is used for the generation of fast-sweeping MMW chirped waveform.

Compared with the typical reported frequency-sweeping lasers, our laser has the unique advantage to provide a narrow ($\sim$10 MHz) instantaneous linewidth during wavelength sweeping, which is a key issue to generate the chirped waveform. Although most of the reported sweeping lasers [23]–[25] exhibit a narrow static linewidth with a much larger wavelength-sweeping range, they may have a very-poor dynamic linewidth ($>$ GHz) during wavelength sweeping. This would result in the wideband MMW white-noise spectra during heterodyne-beating signal generation with optical wavelength sweeping [6]. In addition, compared with the homodyne technique for chirp pulse generation [7], [8], our proposed heterodyne-beating approach should suffer from a larger phase noise of the photogenerated MMW signal. Nevertheless, thanks to the narrow instantaneous linewidth of our sweeping laser, a clear and repeatable instantaneous MMW waveform can be displayed on the very-fast real-time scope, as shown later in Figs. 5 and 6. This result indicates the reasonable good phase noise of our photogenerated MMW signal. To further reduce the phase noise in our proposed scheme, an optical phase-locked loop (OPLL) [7], [26]–[28] with ultrafast response time may be preferred [29] to dynamic locking the phase between two lasers during fast wavelength sweeping.

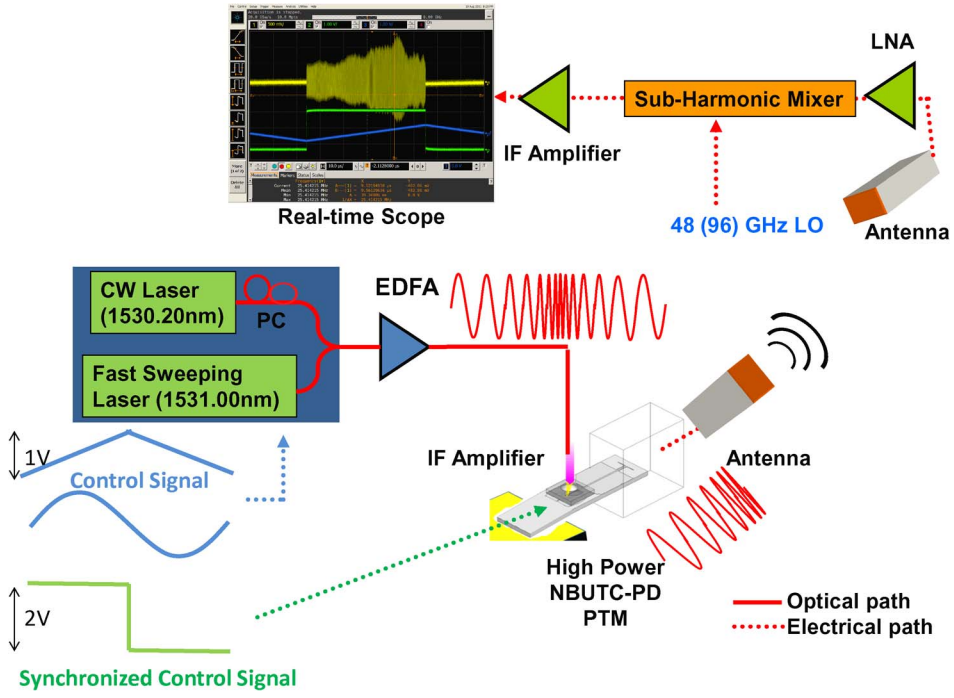

Fig. 1. Measurement setup of our chirped MMW pulse generation system at W-band. LNA: low-noise amplifier. NBUTC-PD: near-ballistic unitraveling carrier photodiode. PTM: photonic-transmitter mixer. EDFA: erbium-doped fiber amplifier. IF Amplifier: intermediate-frequency amplifier.

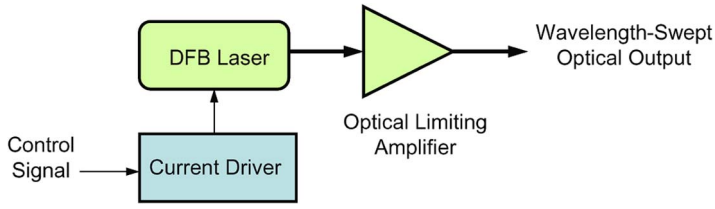

Fig. 2. Block diagram of the tunable DFB-based fast-sweeping laser source.

Fig. 2 shows the conceptual diagram of our fast wavelength-swept laser source. As can be seen, the tunable Distributed-Feedback (DFB) laser in our system ensures a single-frequency output, while the wavelength is tuned by varying the injection current to the DFB chip. During operation, this laser is driven by a small amplitude alternating current (AC) signal source (< 1 V) which allows us to realize optical wavelength scanning and the output amplitude variation of laser is compensated by an optical limiting amplifier [30]. Under AC signal injection, the measured optical spectrum of such narrow linewidth laser would broaden significantly and the 3-dB bandwidth of central linewidth thus corresponds the scanning bandwidth, as discussed latter in Fig. 3(b).

Fig. 3(a) shows the injected peak-to-peak voltage amplitude (V_{pp}) versus the scanning range of optical wavelength. In such measurement, the waveform of the injected AC signal is triangle wave with frequency at 1 kHz. As can be seen, by gradually increasing the V_{pp} from 0.1 V to 1 V, the scanning bandwidth increases from 0.06 and then saturates at 0.12 nm. For the case of central wavelength at 1550 nm, this corresponds to a 14 GHz electrical bandwidth. The maximum operating frequency of injected AC signal is limited at around 10 kHz and the further increase in sweeping frequency (> 10 kHz) would result in a serious decrease in the range of scanning optical wavelengths. The limitation in scanning rate and wavelength range is due to the current driver and

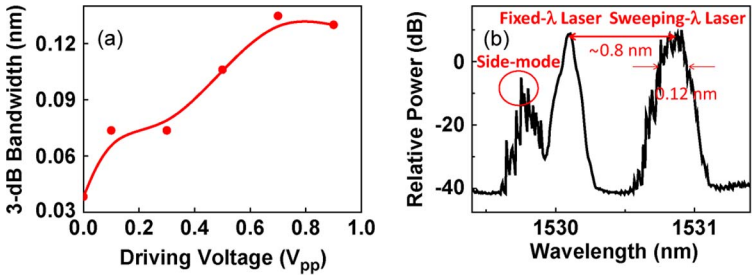

Fig. 3. (a) Peak-to-peak (V_{pp}) amplitude of input AC driving voltage to wavelength sweeping laser versus the 3-dB bandwidth of scanning wavelength. (b) Measured optical spectrum during heterodyne beating measurement for MMW chirped pulse generation. The input V_{pp} is 0.8 V.

the maximum current tolerance imposed by the DFB laser chip. By combining such signal with the output from a fixed-wavelength laser, we can obtain a heterodyne-beating signal with a time-varying beating frequency. To get a linearly chirped pulse, which means that the beating frequency varies linearly with time, we inject the triangle waveform into the sweeping laser and let the separation of two beating optical wavelengths linearly varies with time. If the nonlinearly chirped pulse is preferred, it can be simply generated by using a sinusoidal signal as the control signal of sweeping laser. Furthermore, by properly programming the waveform of control signal of laser, we can directly manipulate the chirped waveform in the transmitter side to efficiently match the response of chirped filter in the receiver end [31]–[33] for high-quality pulse compression. Fig. 3(b) shows the measured optical spectrum during heterodyne-beating measurement (with one fixed wavelength for reference). During such measurement, we injected an AC signal (triangular wave signal) with a frequency at 10 kHz to sweep the central wavelength of our laser. As can be seen in Fig. 3(b), a side-mode exists in the output of such laser during sweeping, which has no significant influence on the heterodyne-beating signal due to the fact that its peak amplitude is much smaller than those of two main modes for beating. In addition, under 1 V_{pp} driving, the measured linewidth of sweeping laser is around 0.12 nm as discussed and we choose the wavelength separation between such two main modes as around 0.8 nm, which corresponds to a $\sim$100 GHz signal with time-varying frequency in our wireless transmission experiment. Overall, by use of this proposed scheme, a truly continuous chirped waveform with excellent tunability, which includes chirped rate, waveform, and central frequency, can be easily realized by changing the waveform and the frequency of AC driving signal of laser. For all the reported photonic chirp microwave pulse generation techniques up to now [7], [8], these issues are all still challenges.

In the transmitter side, we adopted the near-ballistic unitraveling carrier photodiode (NBUTC-PD)-[34]–[36] based broadband and high-power photonic transmitter-mixer (PTM) at around W-band [20], [21]. Fig. 4(a) and (b) show the top-view of such module and its measured and simulated O-E frequency response, respectively.

Details about our device design and processes of simulation can be referred to our previous work [20], [21]. Here, the 0-dB reference point shown in Fig. 4(b) is defined as the output power from an ideal photodiode (i.e., infinite bandwidth) with a 50-Ω load, under an ideal sinusoidal optical source excitation (100% modulation depth), and with the same output photocurrent (4 mA) as that of the PTM during measurement. As can be seen a wide 3-dB O-E bandwidth (67–128 GHz) with a low coupling loss (~ -3 dB) can be achieved simultaneously. The value of coupling loss is defined as the difference between measured MMW power outputs from WR-10 waveguide and the 0-dB reference point, as discussed. As shown in Fig. 1, during the chirped-pulse generation experiment, our PTM is not only illuminated by the optical heterodyne-beating signal but also modulated by voltage square-wave signal, which is synchronized with the driving signal of the sweeping laser, to generate the high-extinction-ratio MMW chirped pulse for free-space radiation [19], [20]. On the receiver side, it is composed of a W-band low-noise amplifier (Millitech, LNA-10-02150), a WR-10 horn antenna, and subharmonic a mixer (VDI diode, WR 10.0 SHM) to down-convert the incoming chirped MMW waveform. The down-converted baseband signal is then amplified and recorded by

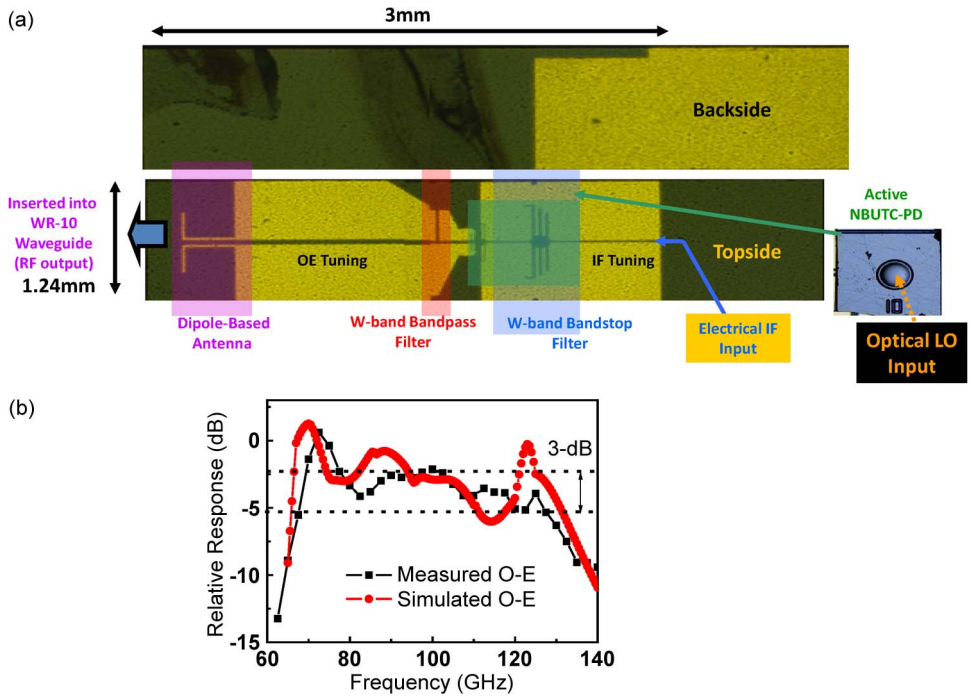

Fig. 4. (a) Top view and backside view of our W-band PTM. (b) The simulated and measured O-E response of our PTM.

an intermediate frequency (IF) amplifier and a 13-GHz real-time scope (Agilent, Infiniium 9000), respectively. The local-oscillator (LO) frequency at 96 GHz was chosen to down-convert the chirped MMW waveform, which ranges from 89 to 103 GHz.

3. Measurement Results

Fig. 5(a)–(c) shows the measured chirped pulse waveform in our receiver end under three different operation conditions. In (a) and (b), the sweeping laser is driving with a triangle waveform (blue line) without and with a square wave (green line) control signal on our transmitter, respectively. In (c), the driving waveform of laser is replaced with a sinusoidal signal for nonlinearly chirped pulse generation, as discussed latter. As can be seen, by applying a square wave as control signal for bias modulation of our transmitter, we can effectively "turn-off" our device, truncate the continuous waveform [as shown in Fig. 5(a)], and get the long time duration (50-μs) pulses. They have high-extinction-ratio and chirped MMW signal inside, which is unclear here due to that we adopted a large time scale ($\sim$ms) on real-time scope to show these long-duration pulses. In addition, the amplitude of generated chirped-waveform in different reference time is nonuniform. Based on the measured O-E response in the interesting band (89–103 GHz), as shown in Fig. 4, the variation in the output power from our transmitter under different operating frequency can almost be neglected. We can thus conclude that the measured nonuniform amplitude of chirped pulse is originated from the variation in output power of our laser during sweeping.

An improved optical equalizer or optical power feedback control circuit integrated with our laser is necessary to further improve the uniformity in amplitude of generated chirped pulse. Nevertheless, we can clearly see that the waveform of each chirped pulse is repeatable under such a large time scale ($\sim$ ms), which implies the feasibility in high quality pulse compression.

Fig. 6(a) shows the measured MMW frequency versus time of detected linearly or nonlinearly chirped waveform in our receiver end. The measurement result clearly indicates that by applying a triangle (sinusoidal) driving signal on sweeping laser a linearly (nonlinearly) relationship between

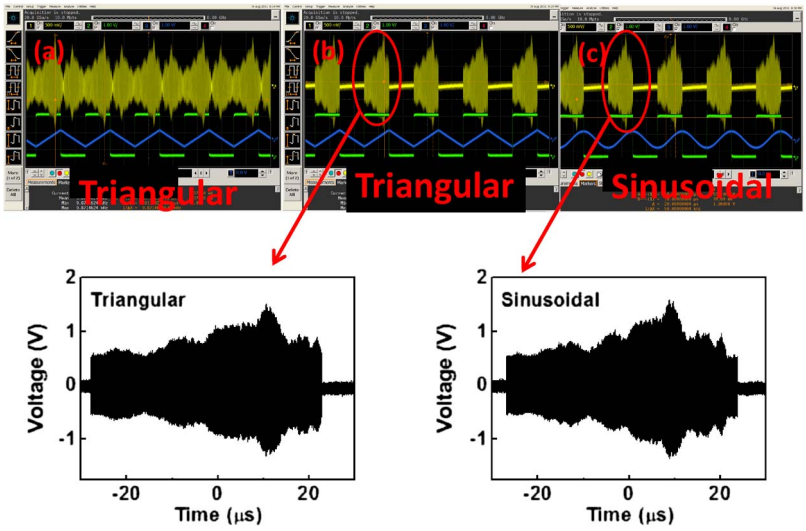

Fig. 5. Triangular [(a) and (b)] and sinusoidal (c) waveform of input AC driving signal to frequency sweeping laser (blue line), the square waveform for bias modulation on PTM (green line), and detected chirped pulse waveform (yellow line). In (a), the square waveform on PTM for bias modulation is turned

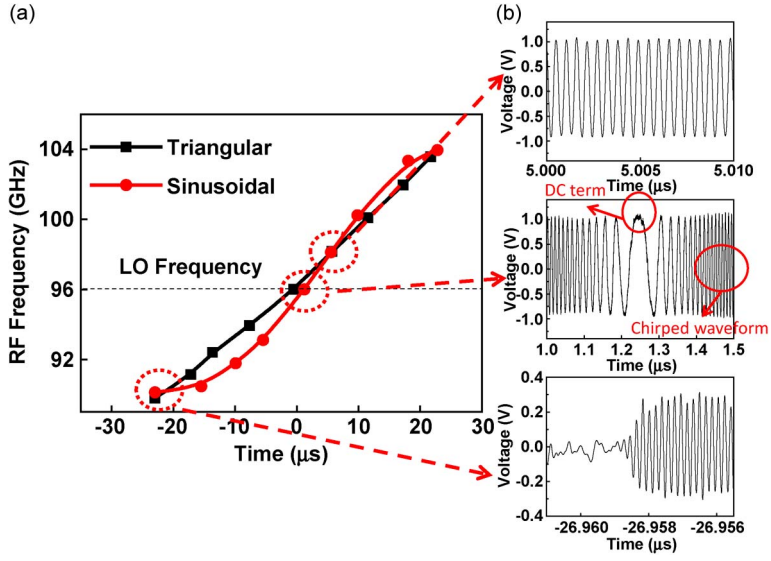

Fig. 6. (a) Measured MMW frequency versus time of our received linearly (black) and nonlinearly (red) chirped pulse. (b) Corresponding measured zoom-in waveform of nonlinearly chirped pulse on real-time scope in different reference time.

time and chirped frequency can be achieved. Fig. 6(b) shows the measured chirped waveform in different time slots, which were recorded on the real-time scope in the receiver-end. During measurement, the MMW LO frequency is fixed at 96 GHz, and we can see that very clear down-converted chirped waveforms are detected. As shown in Fig. 6(b), when the sweeping frequency is near the LO frequency of the mixer (96 GHz), we can see a near DC waveform, and the frequency of generated waveform rapidly increases with sweeping time.

According to our measurement results, we can generate chirped pulse which covers 89–103 GHz with 50 μs sweeping time and the corresponding TBP can be as high as 7×10^5. Such a time-scale (50 μs) of generated chirped pulse is fast enough for long-range remote sensing and detection [1], [2].

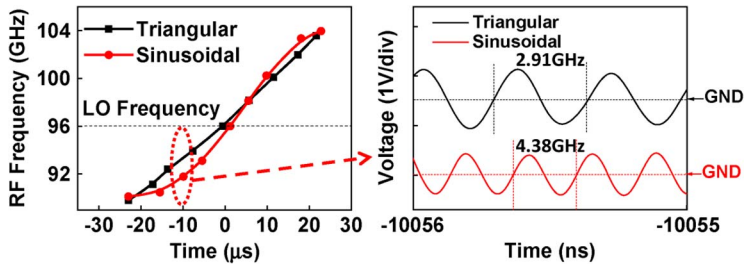

Fig. 7. Detected waveforms of linearly and nonlinearly chirped pulse at the same reference time (-10 μs).

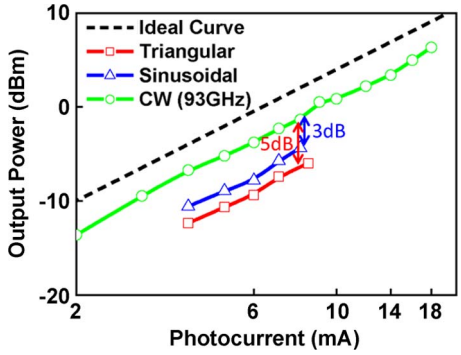

Fig. 8. Measured photogenerated MMW power versus output photocurrent of our PTM under the single-frequency (93 GHz) sinusoidal signal excitation with a 100% modulation depth (green line), nonlinearly (sinusoidal waveform of driving-signal) chirped optical waveform excitation (blue line), and linearly (triangular waveform of driving-signal) chirped optical waveform excitation (red line).

To the best of our knowledge, the achieved TBP is largest ever reported for any kind of chirped pulse generation systems [1]–[5], [8]. Fig. 7 shows the measured linearly and nonlinearly chirped waveform at the same reference time (around -10 μs) after zoom-in for comparison. The measured down-converted intermediate frequency (IF) should equal to radio frequency (RF) by adding the LO frequency at 96 GHz. We can clearly see that clear sinusoidal waveforms with different frequency (2.91 and 4.38 GHz) for linearly and nonlinearly chirped pulse generation can be achieved.

Compared with using the extremely short MMW pulse ($<$ 1 ns) to do the high-(time)-resolution remote sensing, the main advantage of chirped pulse technology is that it can minimize the problem of saturation in front-end MMW amplifier, which is used to amplify the short MMW pulse with a high-peak-voltage for remote-sensing [1]. By use of the demonstrated photonic chirped pulse generation technique here, we may expect that the modulation depth of our heterodyne-beating signal (with time-varying frequency) could be as close as possible to the theoretical maximum value at 100%. Fig. 8 shows the measured photogenerated MMW power versus output photocurrent of our transmitter under different optical excitation schemes.

During such measurement, the square-wave bias modulation signal, which applied onto our transmitter, has been removed. The green trace represents the measurement result of our device under a 100% modulation depth of optical heterodyne-beating signal at a fixed frequency of 93 GHz. Compared with the ideal trace (black dotted line), there is a around 3-dB difference in the output power due to the coupling loss of our device, as discussed in Fig. 4(b). Here, the ideal trace represents the photogenerated MMW power from an ideal photodiode (i.e., infinite bandwidth) integrated with a 50-Ω load, under different values of output averaged photocurrent with a 100% optical modulation depth. This measurement result indicates that the effective modulation depth of optical chirped waveform would be influenced by the waveform of AC driving signal, and in our case, their values are less than 100%. For the case of nonlinearly (sinusoidal signal driving) and linearly (triangle signal driving)

chirped pulse generation, the effective modulation depth is around 71% and 56%, respectively. These results can be attributed to the variation of peak power of central wavelength during wavelength sweeping, as discussed in Fig. 5. The nonequal amplitude of central wavelengths between the fixed wavelength laser and sweeping laser would definitely result in the decrease in modulation depth. Furthermore, as shown in Fig. 3(b), the existence of optical side-mode during sweeping would cause the waste of optical power in the undesired heterodyne-beating frequency components. This is also a possible mechanism that is responsible for the observed degradation in effective modulation depth.

4. Conclusion

In conclusion, we have demonstrated a novel photonic MMW chirped pulse-generation system. By use of the special designed tunable DFB-based wavelength-sweeping laser with a narrow instantaneous linewidth and a broadband/high-power NBUTC-PD-based photonic transmitter, the generation, transmission, and detection of linearly/nonlinearly chirped MMW waveform at W-band, which has a TBP as high as 7×10^5 under a reasonable time scale ($\sim$50 μs) for real-time signal processing, have been successfully demonstrated. To further improve the uniformity in amplitude and effective modulation depth of optical chirped pulse waveform, the improvement in the stability of output optical power during wavelength sweeping of our laser is necessary.

References

[1] M. I. Skolnik, *Radar Handbook*. New York: McGraw-Hill, 1990.
[2] A. W. Rihaczek, *Principles of High-Resolution Radar*. Norwood, MA: Artech House, 1996.
[3] A. Y. Nashashibi, K. Sarabandi, P. Frantzis, R. D. De Roo, and F. T. Ulaby, "An ultrafast wide-band millimeter-wave (MMW) polarimetric radar for remote sensing applications," *IEEE Trans. Geosci. Remote Sens.*, vol. 40, no. 8, pp. 1777–1786, Aug. 2002.
[4] C. Wang and J. Yao, "Large time-bandwidth product microwave arbitrary waveform generation using a spatially discrete chirped fiber Bragg grating," *J. Lightw. Technol.*, vol. 28, no. 11, pp. 1652–1660, Jun. 2010.
[5] R. J. Trew, "Design theory for broad-band YIG-tuned FET oscillators," *IEEE Trans. Microw. Theory Tech.*, vol. MTT-27, no. 1, pp. 8–14, Jan. 1979.
[6] J.-W. Shi, F.-M. Kuo, T. Chiueh, H.-F. Teng, H. J. Tsai, N.-W. Chen, and M.-L. Wu, "Photonic generation of millimeter-wave white-light at W-band using a very-broad-band and high-power photonic emitter," *IEEE Photon. Technol. Lett.*, vol. 22, no. 11, pp. 847–849, Jun. 2010.
[7] J. Yao, "Microwave photonics," *J. Lightw. Technol.*, vol. 27, no. 3, pp. 314–335, Feb. 2009.
[8] J. Yao, "Photonic generation of microwave arbitrary waveforms," *Opt. Commun.*, vol. 284, no. 15, pp. 3723–3736, Mar. 2011.
[9] C.-B. Huang, D. E. Leaird, and A. M. Weiner, "Time-multiplexed photonically enabled radio-frequency arbitrary waveform generation with 100 ps transitions," *Opt. Lett.*, vol. 32, no. 22, pp. 3242–3244, Nov. 2007.
[10] C.-B. Huang, D. E. Leaird, and A. M. Weiner, "Synthesis of millimeter-wave power spectra using time-multiplexed optical pulse shaping," *IEEE Photon. Technol. Lett.*, vol. 21, no. 18, pp. 1287–1289, Sep. 2009.
[11] C. M. Long, D. E. Leaird, and A. M. Weiner, "Photonically enabled agile RF waveform generation by optical comb shifting," *Opt. Lett.*, vol. 35, no. 23, pp. 3892–2894, Dec. 2010.
[12] J. D. McKinney, D. E. Leaird, and A. M. Weiner, "Millimeter-wave arbitrary waveform generation with a direct space-to-time pulse shaper," *Opt. Lett.*, vol. 27, no. 15, pp. 1345–1347, Aug. 2002.
[13] I. S. Lin, J. D. McKinney, and A. M. Weiner, "Photonic synthesis of broadband microwave arbitrary waveforms applicable to ultra-wideband communication," *IEEE Microw. Wireless Compon. Lett.*, vol. 15, no. 4, pp. 226–228, Apr. 2005.
[14] C. Wang and J. P. Yao, "Photonic generation of chirped millimeter-wave pulses based on nonlinear frequency-to-time mapping in a nonlinearly chirped fiber Bragg grating," *IEEE Trans. Microw. Theory Tech.*, vol. 56, no. 2, pp. 542–553, Feb. 2008.
[15] M. Li and J. P. Yao, "Photonic generation of continuously tunable chirped microwave waveforms based on a temporal interferometer incorporating an optically-pumped linearly-chirped fiber Bragg grating," *IEEE Trans. Microw. Theory Tech.*, vol. 59, no. 12, pp. 3531–3537, Dec. 2011.
[16] V. Torres-Company, J. Lancis, P. Andrés, and L. R. Chen, "Reconfigurable RF-waveform generation based on incoherent-filter design," *J. Lightw. Technol.*, vol. 26, no. 15, pp. 2476–2483, Aug. 2008.
[17] R. E. Saperstein, N. Alić, D. Panasenko, R. Rokitski, and Y. Fainman, "Time-domain waveform processing by chromatic dispersion for temporal shaping of optical pulses," *J. Opt. Soc. Amer. B, Opt. Phys.*, vol. 22, no. 11, pp. 2427–2436, Nov. 2005.
[18] A. Hirata, T. Kosugi, N. Meisl, T. Shibata, and T. Nagatsuma, "High-directivity photonic emitter using photodiode module integrated with HEMT amplifier for 10-Gbit/s wireless link," *IEEE Trans. Microw. Theory Tech.*, vol. 52, no. 8, pp. 1843–1850, Aug. 2004.

[19] F.-M. Kuo, J.-W. Shi, J.-H. Huang, N.-W. Chen, M. Rodwell, and J. E. Bowers, "High-power photonic transmitter-mixer with ultra-wide O-E (50 GHz) and IF (26 GHz) modulation bandwidths for wireless data transmission," in *Proc. Int. Top. Meeting Microw. Photon.*, Singapore, Oct. 2011, p. 2137.
[20] F.-M. Kuo, C.-B. Huang, J.-W. Shi, N.-W. Chen, H.-P. Chuang, J. E. Bowers, and C.-L. Pan, "Remotely up-converted 20 Gb/s error-free wireless on-off-keying data transmission at W-band using an ultra-wideband photonic transmitter-mixer," *IEEE Photon. J.*, vol. 3, no. 2, pp. 209–219, Apr. 2011.
[21] N.-W. Chen, H.-J. Tsai, F.-M. Kuo, and J.-W. Shi, "High-speed W-band integrated photonic transmitter for radio-over-fiber applications," *IEEE Trans. Microw. Theory Tech.*, vol. 59, no. 4, pp. 978–986, Apr. 2011.
[22] J.-W. Shi, F.-M. Kuo, N.-W. Chen, C.-S. Goh, D. Wang, S.-Y. Set, and J. E. Bowers, "Photonic generation, wireless transmission, and detection of continuously tunable chirped millimeter-wave waveforms with ultra-high compression ratio at W-band," presented at the Opt. Fiber Commun. Conf. Expo., Los Angeles, CA, Mar. 2012, Paper JW2A.72.
[23] B. R. Biedermann, W. Wieser, C. M. Eigenwillig, T. Klein, and R. Huber, "Direct measurement of the instantaneous linewidth of rapidly wavelength-swept lasers," *Opt. Lett.*, vol. 35, no. 22, pp. 3733–3735, Nov. 2010.
[24] Y. Zhou, K. K. Y. Cheung, Q. Li, S. Yang, P. C. Chui, and K. K. Y. Wong, "Fast and wide tuning wavelength-swept source based on dispersion-tuned fiber optical parametric oscillator," *Opt. Lett.*, vol. 35, no. 14, pp. 2427–2429, Jul. 2010.
[25] R. Huber, M. Wojtkowski, and J. G. Fujimoto, "Fourier Domain Mode Locking (FDML): A new laser operating regime and applications for optical coherence tomography," *Opt. Exp.*, vol. 14, no. 8, pp. 3225–3237, Apr. 2006.
[26] Z.-F. Fan and M. Dagenais, "Optical generation of a megahertz-linewidth microwave signal using semiconductor lasers and a discriminator-aided phase-locked loop," *IEEE Trans. Microw. Theory Tech.*, vol. 45, no. 8, pp. 1296–1300, Aug. 1997.
[27] J.-C. Pearson, P. Chen, and H.-M. Pickett, "Photomixer systems as submillimeter oscillators and coherent test sources," in *Proc. SPIE—Millimeter Submillimeter Detectors Astronomy*, Feb. 2003, vol. 4855, pp. 459–467.
[28] J.-W. Shi, C.-B. Huang, and C.-L. Pan, "Millimeter-wave photonic wireless links for very-high data rate communication," *NPG Asia Mater.*, vol. 3, no. 2, pp. 41–48, Apr. 2011.
[29] S. Ristic, A. Bhardwaj, M. J. Rodwell, L. A. Coldren, and L. A. Johansson, "An optical phase-locked loop photonic integrated circuit," *J. Lightw. Technol.*, vol. 28, no. 4, pp. 526–538, Feb. 2010.
[30] O. C. Graydon, M. N. Zervas, and R. I. Laming, "Erbium-doped-fiber optical limiting amplifiers," *J. Lightw. Technol.*, vol. 13, no. 5, pp. 732–739, May 1995.
[31] M. Bolea, J. Mora, B. Ortega, and J. Capmany, "Chirped microwave photonic filter with high frequency tuning capability," presented at the Opt. Fiber Commun. Conf. Expo., Los Angeles, CA, Mar. 2011, Paper OThA5.
[32] E. Hamidi and A. M. Weiner, "Phase-only matched filtering of ultrawideband arbitrary microwave waveforms via optical pulse shaping," *J. Lightw. Technol.*, vol. 26, no. 15, pp. 2355–2363, Aug. 2008.
[33] E. Hamidi and A. M. Weiner, "Post-compensation of ultra-wideband antenna dispersion using microwave photonic phase filters and its applications to UWB systems," *IEEE Trans. Microw. Theory Tech.*, vol. 57, no. 4, pp. 890–898, Apr. 2009.
[34] J.-W. Shi, C.-Y. Wu, Y.-S. Wu, P.-H. Chiu, and C.-C. Hong, "High-speed, high-responsivity, and high-power performance of near-ballistic uni-traveling-carrier photodiode at 1.55 μm wavelength," *IEEE Photon. Technol. Lett.*, vol. 17, no. 9, pp. 1929–1931, Sep. 2005.
[35] J.-W. Shi, F.-M. Kuo, C.-J. Wu, C. L. Chang, C. Y. Liu, C.-Y. Chen, and J.-I. Chyi, "Extremely high saturation current-bandwidth product performance of a near-ballistic uni-traveling-carrier photodiode with a flip-chip bonding structure," *IEEE J. Quantum Electron.*, vol. 46, no. 1, pp. 80–86, Jan. 2010.
[36] F.-M. Kuo, M.-Z. Chou, and J.-W. Shi, "Linear-cascade near-ballistic uni-traveling-carrier photodiodes with an extremely high saturation-current-bandwidth product," *J. Lightw. Technol.*, vol. 29, no. 4, pp. 432–438, Feb. 2011.